Effect of Intrinsic Properties of Metals on the Adsorption Behavior of Molecules: Benzene Adsorption on Pt Group Metals

Guo-Kun Liu,[†,‡] Bin Ren,*[,†,§] De-Yin Wu,[†] Sai Duan,[†] Jian-Feng Li,[†] Jian-Lin Yao,[‡] Ren-Ao Gu,*[,‡] and Zhong-Qun Tian[†,§]

Department of Chemistry, Xiamen University, 361005 Xiamen, China, State Key Laboratory for Physical Chemistry of Solid Surfaces, Xiamen University, 361005 Xiamen, China, and Department of Chemistry, Suzhou University, 215006 Suzhou, China

Received: January 24, 2006; In Final Form: July 3, 2006

Investigation of benzene adsorption on different metal surfaces closer to a practical system appears to be a very important intermediate stage to utilize the conclusion obtained on single-crystal surfaces. In this paper, we studied the electrochemical adsorption behaviors of benzene on roughened Pt group electrodes using surface enhanced Raman spectroscopy (SERS). The effects of potential, surface roughness, and benzene concentration were investigated. Significant difference in surface Raman spectra of benzene on Ru, Rh, Pd, and Pt surfaces were found. On Pt surfaces, the parallel-chemisorbed benzene, the vertical dissociated chemisorbed benzene, and the physisorbed benzene were observed, evidenced by the ring vibration mode appearing at 872, 1012, and 991 cm^{-1}, respectively. On Pd, only parallel-chemisorbed benzene and physisorbed benzene were found. On Rh and Ru, the SERS signals were mainly from the parallel-chemisorbed benzene, with an extremely weak signal from the physisorbed benzene. The potential dependent study reveals that the parallel-chemisorbed species interacts strongest with the substrate, while the physisorbed species can be easily removed at positive potentials. The models for the adsorbed benzene were given to account for the different types of benzene on these Pt group metals. The difference in the atomization heat of the four metals was used to interpret the different interaction strength of benzene with Pt group metals.

1. Introduction

The interaction between aromatic compounds and various substrates has been and continues to be one of the hot fields in surface sciences since 1970s. As the simplest aromatic molecule, the adsorption behavior of benzene has received much attention. The electronic and geometric structures, work function, and vibrational properties of adsorbate/substrate systems have been studied by various techniques on different surfaces,[1−50] from transition metals surfaces, Mo (110),[1] Co ($10\bar{1}0$),[2,3] Ni (111),[4,5] Ni (110),[6] Ru (001),[7,8] Rh (111),[9−13] rough Rh,[14−16] Pd (111),[17,18] rough Pd,[14−16,19] Ir (111),[20,21] Ir (100),[22] Pt (100),[23−25] Pt (110),[24−26] Pt (111),[4,13,17,25,27−32] rough Pt,[14,33,34] Cu (100),[35] Cu (110),[32] Cu (111),[36,37] Ag,[38−40] Au (111),[41] Au,[42] ZnO (0001),[43] Hg,[44] and bimetallic surface[45] to other surfaces, such as Al (111),[46] Si (111),[47] silica,[48] zeolite,[49] and glassy carbon.[50]

Most of these results show that benzene mainly adsorbs parallel to the metal surface.[2−4,7−21,23,25−33,41−50] Ring distortion has been observed to eliminate ring tension as a result of the interaction of the benzene ring π electron cloud with the surface.[2,3,20,26,29] Three different adsorption sites, bridge, top, and hollow sites, have been proposed for the parallel adsorption configuration.[4,28,32,39]

However, other types of adsorption configurations have also been found. Combined EC-STM and HREELS study has found that benzene is adsorbed slightly tilted with respect to the Pd (111) surface.[18] Benzene has been found to tilt about 20° against the surface due to the lateral interactions among the adsorbed benzene molecules in the first saturatedly adsorbed layer on Cu/Ni(111).[5] Perpendicular adsorption of benzene on silver film has been proposed with use of SERS,[40] which has been identified as benzyne, a dissociated structure of benzene, on Mo (110),[1] Ir (100),[22] Pt (110),[24] and porous Pt.[34] A 1,4-cyclohexadiene-like structure has been suggested to explain the special EEL spectra of benzene adsorbed on Pt (111).[17]

However, it is surprising that different conclusions have been drawn for benzene adsorption, even on the same surface. For example, two different adsorption sites for the parallel mode[4] and 1,4-cyclohexadiene structure for the tilted mode[17] have been suggested for benzene adsorbed on Pt (111), respectively, on the basis of the same EELS results. As a result of the discrepancy, theoretical calculations have been intrigued to investigate the adsorption behaviors of benzene on various surfaces.

Although parallel adsorption configuration has been proposed for benzene on various single-crystal surfaces by several theoretical calculations,[51−58] the preferred adsorption site is different at different surfaces. For example, on Ni (100) and Ni (110), benzene tends to adsorb parallel to the surface in the hollow site, though the bridge site is preferred on Ni (111).[51] On Pd (110), only the parallel mode with a densely packed c (4×2) monolayer has been proposed by STM study.[53] On Pd (111), benzene is flatly adsorbed in the bridge site as revealed by the DFT study.[54] However, using ab initio first principles calculation, similar adsorption energies of the bridge and hollow positions have been obtained for Pd (111) and the same conclusion has been drawn for Rh (111).[55] Both of these studies pointed

* Address correspondence to this author. Fax: +86-592-2085349. E-mail: bren@xmu.edu.cn and ragu@suda.edu.cn.
† Department of Chemistry, Xiamen University.
‡ Department of Chemistry, Suzhou University.
§ State Key Laboratory for Physical Chemistry of Solid Surfaces, Xiamen University.

10.1021/jp060485z CCC: $33.50
Published on Web 08/15/2006

out that the bridge position is the dominant site for the parallel adsorption on Pt (111), which is supported by other calculations that bridge sites are more stable than the hollow sites.[56−58] On Cu (100), the flatly adsorbed benzene will be dissociated in the hollow site producing two dissociated compounds, phenyl and benzyne. Both dissociative products are chemisorbed with the unpaired C atom bonding in the atop site and with the ring standing up in the hollow site, respectively.[52]

The DFT calculation of benzene interacting with Pt and Pt_2 has revealed that low-symmetry equilibrium structures are preferred for benzene−platinum complexes.[59] However, the potential energy surfaces of the benzene−Pt complex revealed two stable structures: a di-π complex and a σ one, three-center two-electron bond C···H···Pt.[60]

Although controversies still exist, the abundant data provided by experimental and theoretical work have allowed us a better understanding of benzene adsorption on various single crystal surfaces in a vacuum. Further extension of such a study is the investigation of benzene adsorption and reaction on rough or nanostructured substrates that are more widely used in practical applications. A systematic study of benzene adsorption and reaction on rough VIIIB metal surfaces will be an important intermediate stage to adopt and use the conclusion obtained from single crystal surfaces in a vacuum and to demonstrate the validity of such conclusions for practical systems. However, in comparison with the study on single crystal surfaces, the studies on rough or nanostructured surfaces are relatively rare. One of the reasons may be the most widely used surface characterization techniques, such as LEED and EELS, are restricted to single crystal surfaces and to UHV conditions. As a very important type of vibrational spectroscopy, surface-enhanced Raman spectroscopy can provide very high detection sensitivity for surface species and can be readily applied to study the rough surface in an electrochemical environment. However, there are only several SERS studies of the interaction between benzene and metal.[15,16,39−41] The reports are even less for Pt-group metals that show unique catalytic properties with a lower SER enhancement (10^2-10^3) than that of noble metals (10^6). Up to now, no direct evidence has been obtained for the adsorbed benzene except for the Weaver group with SERS, who have reported that benzene is adsorbed flatly on Rh and Pd thin layers coated on the SERS-active Au surface.[15,16] Surprisingly, they have not reported any result on Pt, a more important metal in catalysis or electrocatalysis which have been studied in great detail by EELS and IR.

After about 10 years of systematic work, we are now able to extend SERS to several important VIIIB-group transition metals with various surface structures that are especially important in catalysis and electrochemistry as well as other fields of surface science.[61] In the present study, we report a series of studies of benzene adsorption on four Pt-group metals—Ru, Rh, Pd, and Pt—to allow a detailed investigation of the effect of metal substrates in practical systems. Meanwhile, the effect of the electrode potential, the roughness of the electrode, and the concentration of benzene on the adsorption behavior of benzene were systematically studied.

2. Experimental Section

The polycrystalline Pt and Rh rods (diameter 2 mm) were pretreated according to the procedures described elsewhere to achieve SERS activity before being used for electrochemical and Raman study, and the surface roughness was estimated based on the charge of hydrogen adsorption and desorption.[61] The SERS-active Ru surface was prepared by depositing a rough Ru film on a polished polycrystalline Ru electrode at −0.3 V for 30 min in 0.1 M $HClO_4$ solution containing 5 mM $RuCl_3$. The SERS-active Pd or Pt nanoparticle (NPs) electrodes were obtained by dropping a Au core Pd shell (Au@Pd) or Au@Pt NPs onto Pd or Pt electrodes, respectively. The preparation of Au@Pd and Au@Pt NPs has been given elsewhere.[62] Here, 55 nm Au nanoparticles were used as the core, and the thicknesses of Pt or Pd shells were about 5 monolayers, which is already sufficient to make the shell pinhole free. The counter and reference electrodes were a platinum ring and a saturated calomel electrode (SCE), respectively. All solutions were prepared with analytical reagents and Milli-Q water.

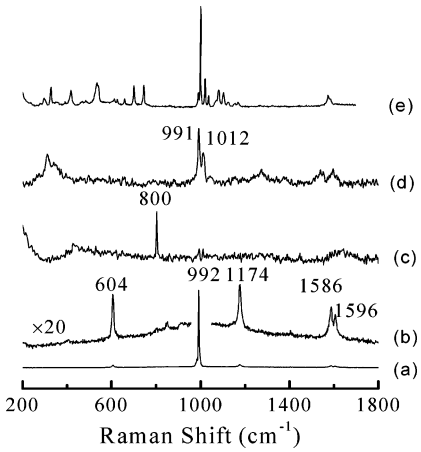

Figure 1. Normal Raman spectra of liquid benzene (a and b) and potential dependent surface Raman spectra on a roughened Pt electrode in 0.1 M KCl solution containing 9 mM benzene at potentials of (c) −1.0, (d) −0.5, and (e) 1.4 V.

Raman spectra were obtained with a LabRam I confocal microprobe Raman instrument (Dilor, France). The excitation line was 632.8 nm from a He−Ne laser. A 50× long working-length objective (8 mm) was used in the present experiment. The electrode potential was controlled with a XD-II potentiostat (Xiamen University, China).

3. Results and Discussion

Figure 1a shows the normal Raman spectrum of liquid benzene and for clarity, it is enlarged by 20-fold and presented as Figure 1b. As can be seen, the strongest signal at 992 cm^{-1} (a_{1g}) from the benzene ring breath vibration with all the other observed bands belongs to e_{2g} modes.

In an electrochemical system, some different spectral features have been observed. Spectra c−e in Figure 1 are the surface Raman spectra obtained on a roughened Pt electrode in 0.1 M KCl solution containing 9 mM benzene with selected potential. At −0.5 V (Figure 1d), the spectrum presents the characteristic of the adsorbed benzene and a detailed analysis will be given in the following section. When the potential was shifted to a very positive or negative potential, drastic change in surface Raman spectra can be found in spectra c and e in Figure 1, which have been investigated in detail by confocal microprobe Raman spectroscopy in our previous studies.[63,64] The results showed that benzene could be reduced to cyclohexane or be substituted to halogen benzene with the change of the electrode potential into the hydrogen adsorption region or the Cl^- oxidation region either in acidic or neutral solutions on these two electrodes. A similar phenomenon was observed on roughened Rh electrodes.

Therefore, to investigate purely the adsorption behavior of benzene, one has to select a suitable potential range to avoid

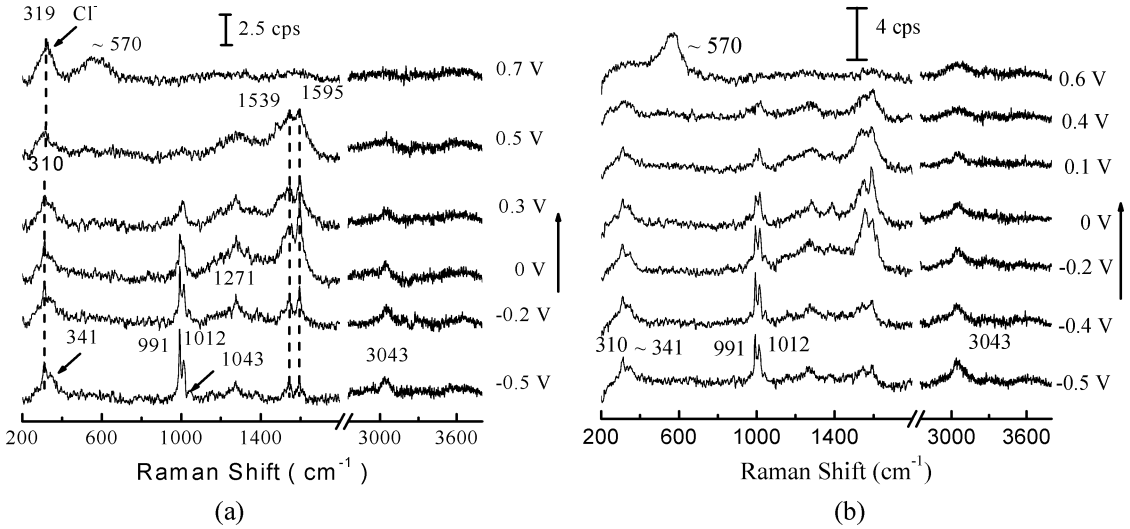

Figure 2. Potential dependent surface Raman spectra on a roughened Pt ($R = 145$) surface in 0.1 M KCl (a) and 0.1 M NaF (b) solutions containing 9 mM benzene, respectively.

the electrochemical reaction of benzene on the electrode surfaces. In our case, we selected −0.5 V for Pt and −0.7 V for Rh, Ru, and Pd electrodes as the initial potential. Then, the potential was moved positively until the occurrence of benzene desorption or metal oxide formation. In the following section, we will concentrate on the adsorption behavior of benzene on Pt electrodes.

3.1. Adsorption of Benzene on a Rough Pt Surface. Figure 2a shows a set of surface enhanced Raman spectra from a roughened Pt electrode (with a roughness factor of 145) in a solution containing 9 mM benzene and 0.1 M KCl. As can be seen in the figure, at −0.5 V, several Raman peaks at around 991, 1012, 1043, 1271, 1539, and 1595 cm^{-1} could be clearly seen in the frequency range of 800−1800 cm^{-1}, possibly related to that of the benzene vibrations. Meanwhile, two peaks at around 310 and 341 cm^{-1} and a peak at around 3043 cm^{-1} were observed in the low and high wavenumber regions, respectively. These peaks show a different relative intensity compared to that of liquid benzene. The intensities of the above-mentioned Raman peaks decrease quickly with the positive shift of the electrode potential; however, no obvious Raman shift can be discerned. When the electrode potential was positively shifted to 0 V, the analysis of the surface Raman spectra becomes difficult and unreliable due to the laser-induced carbonization of surface adsorbates. At 0.5 V, the Raman signal from benzene almost diminished, meanwhile the peak at around 310 cm^{-1} remains almost unchanged. With further positive shift of the potential to 0.7 V, the signal of the adsorbed benzene vanished due to the oxidation of the platinum surface as well as the competitive adsorption of the chloride ion.

To verify the possible competitive adsorption of Cl^- with benzene, we changed the supporting electrolyte to NaF and investigated the potential dependent surface Raman spectra of benzene on the same Pt electrode. The spectra are shown in Figure 2b. The spectra show essentially the same spectral feature as that in KCl solution at potentials negative of 0.1 V, indicating the negligible effect of Cl^- on the adsorption behavior of benzene in this potential region. The band at 310 cm^{-1} in the potential region more positive than 0.5 V in Figure 2a can be assigned to Pt−Cl vibration according to the studies in Cl^- containing solution without benzene.[65,66] Since we also detected the two bands around 310 and 341 cm^{-1} in NaF solution in the potential region more negative than 0.5 V, they should not come from Pt−Cl vibration. Instead, they may originate from different types of Pt−C vibrations.[55] However, on the basis of these data alone, it is impossible to perceive the adsorption configuration of benzene on Pt.

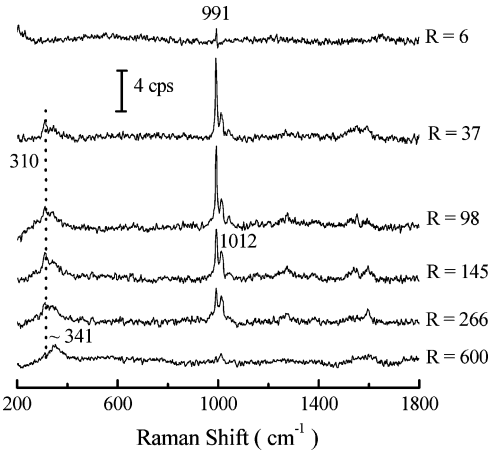

Figure 3. Roughness dependent surface Raman spectra of benzene adsorption on roughened Pt electrodes at −0.5 V in 0.1 M KCl containing 9 mM benzene.

It has been found that surface morphology[67] and concentration of adsorbate[4,32] may influence the adsorption behavior of molecules on the substrates. For a better understanding of the adsorption behavior of benzene on Pt, we carried out a systematic study of this system by changing the roughness of Pt electrodes and benzene concentration.

The surface Raman spectra of benzene on roughened Pt electrodes with different roughnesses are shown in Figure 3. All the spectra were collected at −0.5 V in 0.1 M KCl solution containing 9 mM benzene. When $R = 6$, only a weak peak at ca. 991 cm^{-1} was detected, which is at almost the same position as that observed in solution (990 cm^{-1}). As all the spectra presented in the figure are the subtracted spectra with solution spectrum, therefore, we attribute this signal mainly to the physisorbed benzene. At $R = 37$, the Raman intensity of this peak increases accompanied by a new peak at ca. 1012 cm^{-1} as the shoulder. Meanwhile, a peak assigned to the Pt−C vibration could be clearly seen at ca. 310 cm^{-1} with a broad shoulder at ca. 341 cm^{-1}. At $R = 145$, the intensity of the 991 cm^{-1} peak decreases and that of the 1012 cm^{-1} peak remains almost unchanged. At $R = 600$, the 991 and 310 cm^{-1} peaks could

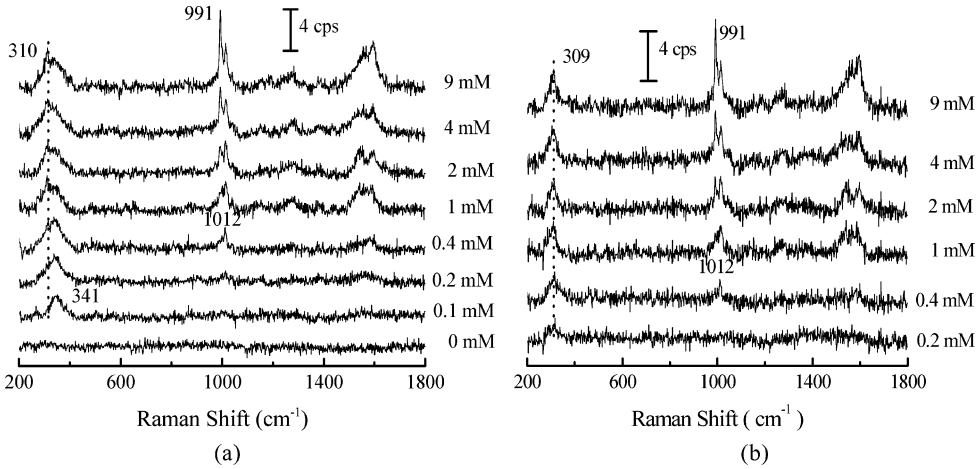

Figure 4. (a) Concentration dependence of surface Raman spectra on roughened Pt electrodes with $R = 145$ in 0.1 M NaF solution at −0.5 V with benzene concentration mentioned in the figure. (b) All spectra were subtracted by Raman spectrum of 0.1 M NaF containing 0.1 mM benzene solution.

hardly be detected and the 1012 cm^{-1} peak becomes fairly weak, meanwhile the 341 cm^{-1} peak still remains quite strong.

It should be mentioned that the roughness dependent surface enhancement effect of roughened Pt electrodes has been studied with pyridine as the probe molecule.[67] It was found that there is an optimal roughness for the highest enhancement. However, we did not find the roughness dependent relative intensity change in the pyridine system. A significant change in the relative intensity in the present case may indicate interesting physical meaning behind the phenomenon. Surprisingly, we did not find any correlation in the intensity of the 991 cm^{-1} peak with that of the two Pt−C vibrations observed in the low-frequency region. Furthermore, we found that the frequency of this peak is only slightly red shifted to that of the solution species (990 cm^{-1}). Both pieces of evidence may indicate that the interaction between the benzene ring and the substrate is very weak and benzene may be physisorbed on the surface. If this assumption is right, then what is the origin of the two Pt−C bands and how are they correlated with the high-frequency modes? How will the benzene concentration influence the spectral feature?

To provide answers to the above questions, we investigated the adsorption of benzene on a roughened Pt electrode with $R = 145$ at different benzene concentrations and the result is shown in Figure 4a. The spectra were acquired at −0.5 V. As has been mentioned above the competitive adsorption of Cl^- is totally suppressed in the negative potential region at a benzene concentration of 9 mM. However, when the benzene concentration becomes very low, we cannot rule out the possible interference of the coadsorbed Cl^- ion. Therefore, to avoid any influence of the Pt−Cl band on the Pt−C band at the very low benzene concentration, we carried out the concentration dependent experiment using a 0. 1 M NaF solution as the supporting electrolyte.

As can be seen from Figure 4a, the Raman spectrum is featureless over the frequency range 200−1800 cm^{-1} when the solution is free of benzene. At a benzene concentration of about 0.1 mM, a broad band at around 341 cm^{-1} can be clearly seen, and the peak at around 1012 cm^{-1} is very weak. At a concentration of 0.4 mM, the 1012 cm^{-1} peak becomes obvious and a weak shoulder at 310 cm^{-1} appears. Meanwhile, the intensity of the peak at 991 cm^{-1} increased steadily with the increasing benzene concentration up to 9 mM (saturated concentration). Interestingly, when the Raman spectra obtained at higher benzene concentrations were subtracted from the Raman spectrum obtained at 0.1 mM, we can clearly see a clear and narrow peak at ca. 309 cm^{-1} (see Figure 4b), though no obvious change can be found for other Raman peaks.

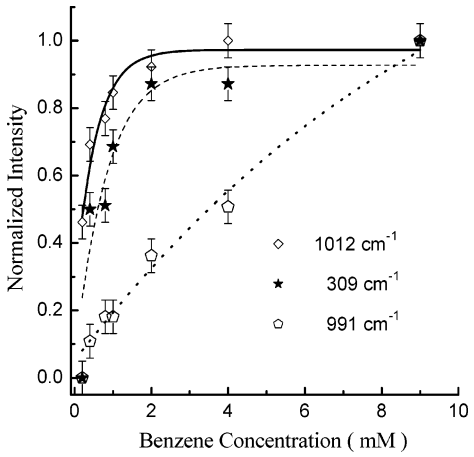

Figure 5. Concentration dependence of the intensities of the Pt−C band and ring breath vibration of benzene adsorbed on a roughened Pt surface.

To see more clearly the dependence of surface Raman bands on the benzene concentration, we plotted the normalized intensities of 309, 991, and 1012 cm^{-1} against the concentration (see Figure 5). Because the spectra are very noisy, the intensities of each band were obtained by Gaussian fitting. As can be seen from the figure, the intensity of the 991 cm^{-1} peak increases almost linearly with the increasing benzene concentration, and meanwhile, the frequency is almost the same as that in solution (990 cm^{-1}). Both indicate that this band is from physisorbed benzene that may not directly interact with the metal surface. Therefore, it is reasonable to observe that this peak is very sensitive to the applied potential and can be easily removed from the solid/solution interface with the positive shift of the potential, as shown in Figure 2. A detailed discussion on the formation of the physisorbed species will be given later.

Also in Figure 5, we could clearly find that the 309 and 1012 cm^{-1} peaks follow essentially the same trend with concentration, indicating that they may be from the same species. It should be pointed out that in one of our previous papers, we tentatively assigned the 1012 cm^{-1} band to the b_{1u} mode for the parallel adsorbed benzene.[68] This mode also shows a peak at around 1012 cm^{-1} and is related to the ring triangular vibration, a Raman inactive mode. We have assumed that this band might become Raman active after the benzene molecule is adsorbed

TABLE 1: Ring Breath Vibration Mode of Different Substituted Benzenes

sample	ring breath mode (cm^{-1})	sample	ring breath mode (cm^{-1})
C_6H_6	992	$C_6H_4(NO_2)_2$	1035
C_6H_5I	996	$C_6H_4Cl_2$	1036
C_6H_5Br	998	C_6H_4ClBr	1037
C_6H_5CN	999	$C_6H_4ClCH_3$	1042
$C_6H_5CH_3$	1001	$C_6H_4BrCH_3$	1044
C_6H_5Cl	1003	$C_6H_4(OCH_3)_2$	1048
C_6H_5F	1008	$C_6H_4(CH_3)_2$	1053

at the surface due to the symmetry degradation. However, this assignment seems incorrect after the deuteration experiment with d_6-benzene, because we found that this peak only red shifted to 1001 cm^{-1} instead of 970 cm^{-1} as expected.[69] Therefore, this band may not come from the ring triangular mode, but from another vibrational mode.

To find out the origin of the 1012 cm^{-1} mode, we list in Table 1 the ring breath modes of different substituted benzenes.[70] It can be clearly found that the ring breath mode of benzene blue shifts when one or two of the H atoms are substituted by other functional groups. For example, the band will blue shift from 992 cm^{-1} (C_6H_6) to 1008 cm^{-1} (C_6H_5F) or even severely blue shift to 1053 cm^{-1} ($C_6H_4(CH_3)_2$). It was found that the weaker the electron donation ability of the substituting group is, the larger the blue shift of the ring breath mode will be. The electron structure of the Pt atom is $5d^96s^1$ and the Pt atom is normally considered as an electron acceptor. Therefore, if we assume that benzene is adsorbed on the Pt surface with one of its hydrogens lost to form C_6H_5Pt, leading to dissociated adsorption of benzene, it is reasonable to understand the blue shift of the ring breath mode of benzene to 1012 cm^{-1} on the basis of the data listed in Table 1. A simple theoretical calculation with the B3LYP method showed that the ring breath mode blue shifts from 978 cm^{-1} (C_6H_6) to 1006 cm^{-1} (C_6H_5Pt), which is supportive of the above assumption.[71] Evidence for such a dissociated chemisorption has been observed for phenyl iodide adsorbed on Mo_2C/Mo (111). It was found that the ring breath mode blue shifted from 997 to 1012 cm^{-1} when phenyl iodide was adsorbed on this surface to form the C_6H_5 structure.[72] Therefore, we can convincingly assign the 1012 cm^{-1} peak to the benzene ring breath mode with the benzene ring perpendicular to the surface and the 309 cm^{-1} peak to the Pt−C vibration of such adsorbed species. This adsorption configuration makes the ring breath mode one of the strongest vibration modes in surface Raman spectra according to the surface Raman selection rule. Furthermore, on the blue side of the 1012 cm^{-1} peaks, a weak band at around 1043 cm^{-1} can be observed, which can be assigned to the C−H in-plane bending.[69] However, we cannot exclude the possibility that this band may be related to ring breath vibration of the adsorption structure of $C_6H_4Pt_2$ with two of the hydrogen atoms lost, according to Table 1 and the discussion on the 1012 cm^{-1} peak. This assignment is supported by some previous studies of various substrates.[1,22,24,34]

It can be seen from Figure 4a, at a low benzene concentration, that there is only one broad peak at ca. 341 cm^{-1} and we could not detect any other signal accompanying this band. Although we have tentatively assigned it to Pt−C vibration according to the literature,[55] why could we not detect the counterparts in the high-frequency region? It should be especially pointed out that the intensity of this band only slightly decreased even after the Pt electrode had been cleaned in 0.5 M H_2SO_4 solution until the recovery of the characteristic cyclic voltammogram after the in situ Raman experiment. This indicates the adsorbed species related to this Pt−C must have a very strong interaction

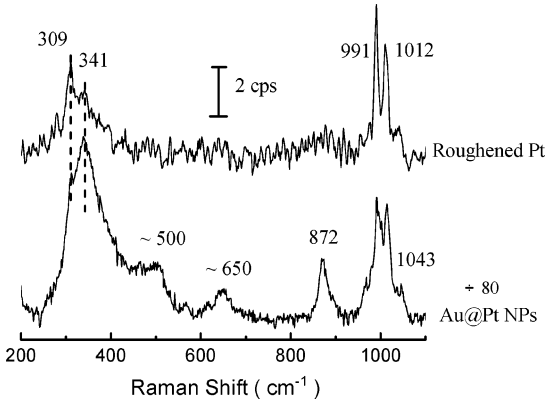

Figure 6. Surface Raman spectra of benzene adsorbed on roughened Pt and Au@Pt NPs surfaces at −0.5 V in 0.1 M KCl containing 9 mM benzene.

with the Pt surface and is very hard to remove with the traditional electrochemical cleaning process. We may assume that the surface coverage of this species on the Pt electrode is very low because of the negligible effect of this adsorbed species on the cyclic voltammogram of the Pt electrode and the independence of the surface Raman intensity of the 341 cm^{-1} peak (Figure 4a) on the concentration of benzene.

To find out the origin of this band, we investigated the adsorption of benzene using a substrate that may provide higher surface enhancement, i.e., a Au core Pt shell (Au@Pt) nanoparticles-assembled electrode, as the SERS substrate.[62] Such a substrate has the chemical properties of the Pt, whereas it is supportive of high SERS activity boosted by the high electromagnetic field enhancement of the Au core. Figure 6 shows SER spectra of benzene adsorbed on a Au@Pt NPs surface and a roughened Pt surface at −0.5 V in 0.1 M KCl containing 9 mM benzene. The intensity of the former spectrum has been scaled down by a factor of 80 to allow for comparison. Apparently, the spectrum obtained on the Au@Pt substrate shows a much higher signal-to-noise ratio, which allows us to observe the weak peaks in the frequency region between 400 and 900 cm^{-1} that is too weak to be observed on pure Pt surfaces. The bands at around 500 and 650 cm^{-1} could be assigned to the C−C−C out-of-plane bending and C−H out-of-plane bending, respectively.[16,55,69] The band at around 872 cm^{-1} can be assigned to the benzene ring breath vibration for benzene adsorbed parallel on the Pt surface, which is in good agreement with the theoretical calculation showing a frequency at 826 cm^{-1}.[55] According to the good correlation in the intensities of 872 and 341 cm^{-1} bands, we can assign the 341 cm^{-1} to the Pt−C vibration of this parallel adsorption mode. In the two Pt−C bands detected, the band related to the parallel mode has a higher frequency compared with the vertical one, indicating that the parallel adsorbed benzene has a stronger interaction with the Pt substrate, possibly due to a better electron cloud overlap between the π electron of the benzene ring and the d orbitals of the Pt atom.

In the literature, two different sites, top and hollow, have been proposed for benzene parallel adsorbed on Pt (111) on the basis of EELS and RAIRS results, in which two pairs of the out-of-plane C−H bending, 820 and 920 cm^{-1} or 829 and 900 cm^{-1}, have been observed, respectively.[4,32] However, in our SERS study, only one broad band at 872 cm^{-1}, assigned to the ring breath mode, was detected. Our result indicates that there is only one configuration for the parallel-adsorbed benzene, instead of the two types of adsorption configuration on single-crystal surfaces. The different selection rules for Raman, EELS, and RAIRS may account for the obvious difference in the

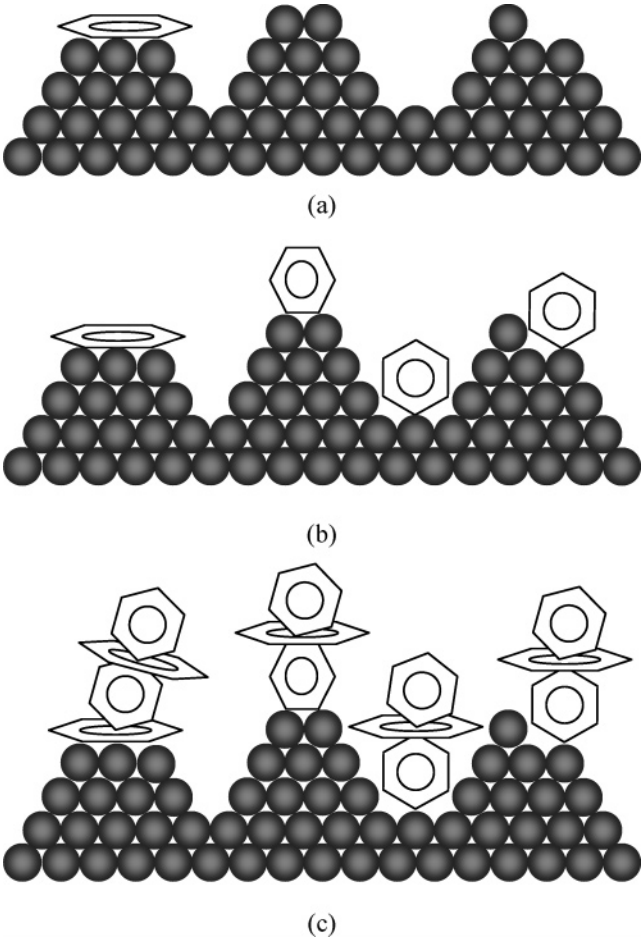

Figure 7. Schematic models of benzene adsorption on a roughened Pt electrode with the increasing benzene concentration from parts a to b to c.

observed signal obtained with different techniques. For instance, benzene is a molecule with central symmetry, therefore, the IR active mode will be Raman inactive, and vice versa. Also accounting for this may be a more complicated environment in electrochemical systems compared with that of vacuum and a more random surface structure of a roughened surface compared with that of a single-crystal surface.

Surprisingly, it can be found in Figure 6 that the relative intensities of the parallel-chemisorbed benzene to the vertical dissociative adsorbed benzene on these two substrates are different. The main reason may still be the same as revealed already in the roughness dependent experiment, which shows that the morphology of substrate plays an important role in influencing the adsorption behavior of benzene.

Since all the detected bands can be assigned clearly, it is now worthwhile for us to reexamine concentration dependent data to extract information about the adsorption configuration. Figure 7 shows the schematic diagram of the models proposed for the possible configurations observed in this study. At a low benzene concentration (up to 0.1 mM), there are enough suitable surface sites for the benzene molecule to adsorb parallel to the surface (see Figure 7a), showing only one Pt−C band around 341 cm^{-1}. With the increase of the concentration, the surface concentration of the parallel mode is already too high to accommodate more benzene molecules to adsorb parallel, therefore some of the benzene molecules may interact directly with one or two hydrogen atoms cleaved and be dissociated to adsorb vertically or tilted on the surface (see Figure 7b) showing bands at 310 and 1012 cm^{-1}. When the concentration is higher than

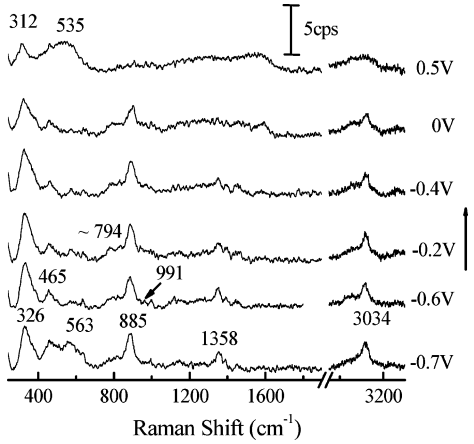

Figure 8. Potential dependent surface Raman spectra on a roughened Rh electrode in 0.1 M KCl solution containing 9 mM benzene.

4 mM, the intensity of this type of benzene will not change, indicating a saturated adsorption for this type of benzene. However, the almost linear increase in the intensity of the band at 991 cm^{-1} indicates the amount of physisorbed benzene also increases linearly with concentration. The fact indicates the formation of a multilayer of benzene for such an adsorption mode. In a recent theoretical calculation of benzene dimers, it was pointed out that benzene molecules tend to interact with their ring planes perpendicular to each other.[73] Experimentally, it was also found that a layer-by-layer crystalline phase can be formed for benzene physisorbed on the Ru (001) surface, with the ring plane in one layer vertical to another one for the first several layers.[7,8] Accordingly, the benzene molecules in each layer are perpendicular to that in neighboring layers (see Figure 7c).

After exploring the concentration and roughness effect, it may be worthwhile to find the effect of the substrate on the adsorption behavior of benzene.

3.2. Adsorption of Benzene on Rough Rh, Ru, and Pd Surfaces. Figure 8 shows the potential dependent surface Raman spectra of benzene adsorbed on an electrochemically roughened Rh electrode in 0.1 M KCl solution containing 9 mM benzene. Compared with the normal Raman spectrum of liquid benzene (Figure 1), the surface Raman spectra of benzene on the Rh surface change greatly, showing bands at ca. 326, 465, 563, 885, 1345, and 3034 cm^{-1} and a shoulder at ca. 794 cm^{-1}. According to the discussion of the Pt system, the peak at around 326 cm^{-1} can be convincingly ascribed to the Rh−C vibration with control experiments in solutions free of Cl^- and the EELS and SERS results.[12,16] All other peaks can be related to that of the parallel-chemisorbed benzene. All these peaks are weakened with the positive shift of the electrode potential and diminish at 0.5 V, where oxidation of the Rh surface and the competitive adsorption of Cl^- occur. With the positive shift of the potential, the position and the relative intensity of surface Raman peaks only changed slightly, indicating little effect of the electrode potential on the adsorption configuration of the benzene molecule.

Similar phenomena were observed on Ru and Pd surfaces. The Ru electrode was prepared by electrochemical deposition and the Pd electrode was prepared by dispersing the palladium shell gold core nanoparticles over a Pd electrode (Au@Pd). Figure 9 shows the surface Raman spectra of benzene obtained from Ru and Pd surface at −0.7 V, and for the convenience of comparison the spectra obtained on Rh and Pt (Au@Pt) are also presented (note that the spectra obtained from Pd and Pt have been scaled down by 20- and 40-fold, respectively). It can be seen from the figure that the surface Raman spectrum from the

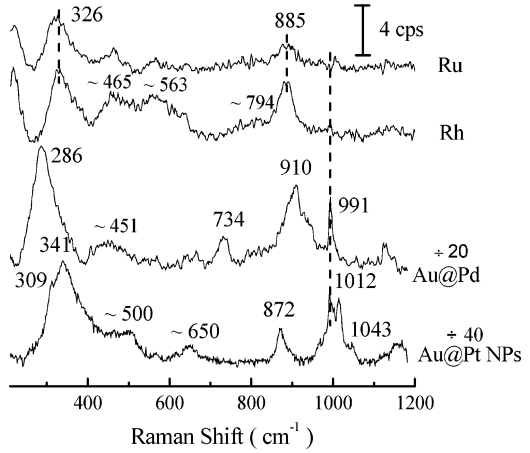

Figure 9. Surface Raman spectra of benzene adsorption on roughened Ru, Rh, and Au@Pd NPs surfaces at −0.7 V and on Au@Pt NPs surface at −0.5 V in 0.1 M KCl solution containing 9 mM benzene.

Ru surface is similar to that from the Rh surface except at a lower intensity. However, the SER spectrum obtained on the Pd surface is very different from that of the former two electrodes, showing bands at 286, 451, 734, 910, and 991 cm^{-1}, with features similar to that on Pt. Similarly, the peak at 991 cm^{-1} can also be assigned to the ring breath vibration of the physisorbed benzene. On Pt and Pd surfaces, the 991 cm^{-1} peak is quite strong while it is a very weak peak on the Rh and Ru surfaces, which means that the coverage of the physisorbed benzene on Pt and Pd is quite high. The peak at around 286 cm^{-1} can be assigned to the Pd−C vibration.[55]

It should especially be pointed out that we observed peaks at 3034 cm^{-1} (C−H vibration of benzene) and 2267 cm^{-1} (C−D vibration of deuterated benzene), which is contradictory to that reported by Zou et al. on the adsorbed benzene on Rh and Pd surfaces.[16] They ascribed the reason for the absence of C−H and C−D bands to the fact that benzene is adsorbed with the ring parallel to the surfaces, thereby they will be Raman-inactive according to the surface selection rule.[15] Analyzing the results of our two groups, we would rather ascribe the reason for the absence of Raman peak of C−H and C−D to the low detection sensitivity of the CCD they used in the longer wavelengths.[16] Therefore, it is not proper to use only the C−H (D) band to determine the orientation of benzene on metal surfaces.

For a better analysis of our result, we listed in Table 2 the vibrational data for the adsorbed benzene on Pt, Rh, Pd, and Ru surfaces from the literature (including experimental data and theoretical calculations).[12,16,55] Due to the size limitation of the table, only the vibrational modes that have been detected in SERS are listed. The bands of the liquid benzene and the corresponding vibrational assignments are also given with the ratio of ν_H/ν_D listed in parentheses for a better comparison. It can be seen from Table 2 that only out-of-plane vibrational modes could be detected on Rh (111) by using EELS and they were greatly enhanced compared with the in-plane modes on rough Rh and Pd surfaces with SERS. It is well-known that in EELS only those vibrational modes with dynamic dipole components perpendicular to the metal surface could be observed,[4,12] whereas in SERS those vibrational modes with polarizability tensors normal to the metal surface could be greatly enhanced.[15] Therefore, both of the experimental results indicate that benzene is parallel adsorbed on both the single-crystal surfaces and rough surfaces according to the surface selection rules of EELS and SERS, which is further evidenced with theoretical calculations.[55]

Examining Figure 9 again, we will find that the parallel-chemisorbed benzene gives a wider band compared with the

TABLE 2: Comparison of Vibrational Frequencies (cm^{-1}) for Normal Modes of Benzene Adsorbed on Various Metal Surfaces from Experiments and Calculations

description[69]	mode	liquid[16,69]	Pt (111)[a]	SERS on Pt	SERS on Au@Pt NPs	Rh (111)[a]	Rh (111)[b]	SERS on deposited Rh[16]	SERS on Rh and Ru	SERS on deposited Pd[16]	Pd (111)[a]	SERS on Au@Pd NPs
M−C stretching	ν_{M-C}		327, 352	310 (1.00) 341 (1.00)	310 341	351	550 (1.00) 345 (1.05)	355 (1.05)	326 (1.00)	~250	289	286
C−C−C out-of-plane bending	$\nu_{16}(e_{2u})$	398 (1.15)	501		~500	479		~495 (1.12)	461 (1.07)	~430	455	451
C−C−C in-plane bending	$\nu_6(e_{2u})$	606 (1.05)	566			546		~605	563 (1.00)	590	551	
C−H out-of plane bending	$\nu_{11}(a_{2u})$	673 (1.36)			~650			~795 (1.42)	794 (1.26)	~735		734
ring breath	$\nu_1(a_{1g})$	992 (1.05)	826	991 (1.05) 1012 (1.01)	872, 991, 1012	870	880 (1.05)	970/885 (1.05)	878 (1.02)	955/930 (1.05)	881	910/991
C−H in-plane bending	$\nu_{18}(e_{1u})$	1037 (1.03)		1043	1043							
C−H in-plane bending	$\nu_3(a_{2g})$	1350 (1.28)						1350 (1.29)				
C−C stretching	$\nu_{14}(b_{2u})$	1309 (1.02)		1271 (1.05)			1320 (1.0)		1356 (1.00)			
C−H stretching	$\nu_2(a_{1g})$	3062 (1.34)	3042	3043 (1.22)		3060	~3000 (1.33)		3034 (1.34)		3060	

[a] Reference 55. [b] References 12 and 16.

physisorbed benzene, a marked shift in the vibrational frequency, and a significant change in the relative intensity. For example, the ring breath mode is significantly broadened accompanied by a red shift in the frequency. Both phenomena indicate a strong interaction between the benzene ring and the substrates. The decrease of the relative Raman intensity of the ring breath vibration (885 cm^{-1}) to the C−H stretch vibration (3034 cm^{-1}) from 8:1 to 1.3:1 after being adsorbed on Ru and Rh surfaces indicates that benzene is adsorbed parallel to the surface. On the basis of the above results, one might conclude that the benzene molecule is adsorbed parallel on these three surfaces. As a result, benzene may interact strongly with the metal surface, which leads to a decrease in the π electron density of the benzene ring and consequently results in a large red shift of the frequency of the ring breath vibration of benzene. The strong interaction makes the C−H bonds flip out of the molecule plane, which allows an effective interaction of this mode with the electric field perpendicular to the substrate, giving an observable surface Raman signal of the C−H in-plane vibration appearing at around 3034 cm^{-1}, shown in Figure 8. Such kind of parallel adsorption has been demonstrated by a theoretical calculation of Pd (111) and Rh (111) surfaces,[55] and is consistent with the results on single-crystal surfaces, such as Ru (001),[7] Pd (111),[18] and Rh (111).[14−16] Then, what is the reason for a smaller red shift of the ring breath vibration for benzene chemisorbed on the Au@Pd surface?

3.3. Comparison of the Parallel Adsorption of Benzene on Different Metal Surfaces. In both our own study on Pt, Ru, Rh, and Pd surfaces and in reported results on Ag[38] and Au[42] surfaces of the parallel-chemisorbed benzene molecule, different frequency has been observed for the ring breath vibration in SER spectra. For example, the ring breath mode for a free benzene molecule in an aqueous solution is about 990 cm^{-1}; however, it red shifts to 986 cm^{-1} (Ag),[38] 973 cm^{-1} (Au),[42] 910 cm^{-1} (Pd), 885 cm^{-1} (Ru and Rh), and further to 872 cm^{-1} (Pt). The tendency agrees well with the theoretical calculation: 881 cm^{-1} (Pd (111)), 870 cm^{-1} (Rh(111)), and 826 cm^{-1} (Pt (111)).[55] Meanwhile, the M−C vibration blue shifts from 286 cm^{-1} for Pd−C, to 326 cm^{-1} for Ru−C and Rh−C, and to 341 cm^{-1} for Pt−C. Both a larger red shift of the ring breath vibration and a higher M−C frequency indicate a stronger interaction between benzene molecules and the substrate. Therefore, we will see that the interaction between benzene and the metal decreases in the order of Pt, Ru and Rh, Pd, Au and Ag. Then, what makes the difference?

Brewer−Engel valence-bond theory,[74] derived from valence-bond theory, describes the origin of the different strengths of the metal bonds. It is concluded that although all the valence electrons contribute to the bonding in the transition metal, the s and p electrons determine the long-range structure and the d electrons determine the short-range bonding,[17] and the difference in the bonding of the d electrons determines the strength of the metal bonds, which could be quantitatively expressed as the value of ΔH (the heat of atomization of metals), a sensitive function of d orbital filling of and periodic row of transition metals.[17,74] Furthermore, the theory has been extended empirically to interpret surface phenomena, such as the different interaction between metal and adsorbate,[17] which is determined by the overlap between d orbitals of metal and the molecular orbitals of adsorbate: the greater the overlap, the stronger the interaction.

This theory has been employed by Grassian et al. to explain the different EELS results of benzene adsorption on the (111) surface of Ag, Pd, Ni, Rh, and Pt.[17] The interaction between benzene and metal increases in the order of Bz-Ag[17] < Bz-Pd[17] < Bz-Ni[4] < Bz-Rh[12] < Bz-Pt,[4] which could be further semiquantitatively related by the different values of ΔH (atomization energy) of these metals.[17,74] Similarly, this theory may also be employed to explain the difference in the SER spectra on different metal surfaces.

For the convenience of analysis, the frequency of the ring breath mode of benzene was used as an indicator of the strength of the benzene−metal interaction: the larger the red shift of this mode, the stronger the interaction between benzene and metal. Then, the interaction between benzene and the six rough metals mentioned above increases in the order of Bz-Ag < Bz-Au < Bz-Pd < Bz-Rh (Bz-Ru) < Bz-Pt. On the basis of Brewer−Engel valence-bond theory,[74] the orbital diffuseness for the 5d orbitals of Pt metal is much greater than that for the 4d orbitals of Rh and Pd metals, which makes the interaction between benzene and Pt metal the strongest due to a maximal overlap of the benzene π electron cloud and the Pt 5d orbitals. The reason for a weaker interaction between benzene and Pd is due to its $4d^{10}$ structure, which is hard to overlap with the benzene π electron cloud compared with Rh $4d^8$ orbitals. For Ag, the $4d^{10}$ $5s^1$ electron structure makes the least overlap of Ag 4d orbitals with the benzene π electron cloud. As a result, the benzene ring structure was the least distorted and the blue shift of the out-of-plane bending mode is also the smallest for Ag. This tendency could also be further semiquantitatively related with the different values of ΔH (atomization energy) of these metals:[17,74] 69 kcal/mol (Ag) < 88 kcal/mol (Au) < 91 kcal/mol (Pd) < 133 kcal/mol (Rh) < 135 kcal/mol (Pt) < 153 kcal/mol (Ru). The abnormal ΔH value of Ru may be due to a different crystal structure, hexagonal close-packed, in comparison with the cubic close-packed structure for the other metals.[74]

As a result, the dissociated species formed on a rough Pt surface may be due to the strong interaction between benzene and Pt. Through detailed comparison of the results obtained from the well-defined single-crystal surfaces[4,12,17] and the ill-defined rough surfaces either from references[38,42] and our own results, a similar adsorption configuration and the same tendency of the interaction between benzene and metals is found. Interestingly, although the SERS results are obtained on rough surfaces at the liquid/metal interface, an environment much more complicated than that of the gas/metal interfaces, we can still determine that the intrinsic property of metal plays an important role on molecule adsorption on a metal surface, no matter whether the surface structure is well- or ill-defined.

4. Conclusion

In summary, we report a systematic SERS study of benzene adsorption on different Pt group metals, including Pt, Pd, Rh, and Ru, with the consideration of benzene concentration, surface morphology, and potential effect. The concentration dependent study has revealed that benzene can exist on the Pt surface in at least three forms: (1) parallel-chemisorbed benzene that interacts with the metal surface via the π electrons of the benzene ring and with a large red shift (over 100 cm^{-1}) in the ring breath vibration and Pt−C at 341 cm^{-1}; (b) vertical or tilted dissociated chemisorbed benzene that interacts with the metal surface by cleaving one or two of the six hydrogens with a small blue shift (ca. 20 cm^{-1}) in the ring breath vibration and a Pt−C at 310 cm^{-1}; and (c) multilayer physisorbed benzene that is adsorbed through the chemisorbed benzene either parallel or vertical to the surface, showing ring breath vibration with a frequency close to that of the free benzene molecule. Three models have been proposed to account for these three types of adsorbed benzene.

It was found that the parallel-chemisorbed benzene has a stronger interaction with the Pt substrate compared with the vertical chemisorbed one as evidenced by a larger red shift of the ring breath vibration and higher frequency of the Pt−C vibration. In addition, a quite remarkable effect of the metal substrate on the benzene adsorption has been found. Different from the result on Pt, on Pd, Rh, and Ru surfaces, the parallel-chemisorbed species are the dominant surface species, with a decreasing amount of physisorbed species. Even for the parallel-chemisorbed species, the red shift of the ring breath vibration decreases in the order of Pt, Rh and Rh, and Pd, which has been well explained by the different d orbital electron structures of the four metals. It should be pointed out that although the study was carried out on rough surfaces, the distinct effect of metal on the adsorption behavior of benzene on different metal surfaces can still be found and the main result is still consistent with that obtained on single-crystal surfaces. In a separate paper, we will further demonstrate the effect of the substrate on the competitive and cooperative adsorption of benzene and other molecules and ions on Pt and Rh surfaces.

Acknowledgment. This work has been supported by the Natural Science Foundation of China (20433040, 90206039, and 20373046), Ministry of Education of China (20040384010 and NCET-05-0564), Fok Ying Tung Educational Foundation (101015), and 973 Project (2001CB610506).

References and Notes

(1) Liu, A. C.; Friend, C. M. *J. Chem. Phys.* **1988**, *89*, 4396.
(2) Barnes, C. J.; Valden, M.; Pessa, M. *Surf. Rev. Lett.* **2000**, *1*, 67.
(3) Pssi, K.; Lindroos, M.; Barnes, C. J. *Chem. Phys. Lett.* **2001**, *341*, 7.
(4) Lehwald, S.; Ibach, H.; Demuth, J. E. *Surf. Sci.* **1978**, *78*, 577.
(5) Koschel, H.; Held, G.; Trischberger, P.; Widdra, W.; Steinruck, H. P. *Surf. Sci.* **1999**, *437*, 125.
(6) Kang, J. H.; Toomes, R. L.; Robinson, J.; Woodruff, D. P.; Schaff, O.; Terborg, R.; Lindsay, R.; Baumgartel, P.; Bradshaw, A. M. *Surf. Sci.* **2000**, *448*, 23.
(7) Jakob, P.; Menzel, D. *Surf. Sci.* **1989**, *220*, 70.
(8) Jakob, P.; Menzel, D. *J. Chem. Phys.* **1996**, *105*, 3838.
(9) Lin, R. F.; Koestner, R. J.; Van Hove, M. A.; Somorjai, G. A. *Surf. Sci.* **1983**, *134*, 161.
(10) Koel, B. E.; Somorjai, G. A. *J. Electron Spectrosc.* **1983**, 287.
(11) Neumann, M.; Mack, J. U.; Bertel, E.; Netzer, F. P. *Surf. Sci.* **1985**, *155*, 629.
(12) Koel, B. E.; Crowell, J. E.; Mate, C. M.; Somorjai, G. A. *J. Phys. Chem.* **1984**, *88*, 1988.
(13) Mate, C. M.; Somorjai, G. A. *Surf. Sci.* **1985**, *160*, 542.
(14) Schmiemann, U.; Jusys, Z.; Baltruschat, H. *Electrochim. Acta* **1994**, *39*, 561.
(15) Zou, S. Z.; Williams, C. T.; Chen, E. K. Y.; Weaver, M. J. *J. Am. Chem. Soc.* **1998**, *120*, 3811.
(16) Zou, S. Z.; Williams, C. T.; Chen, E. K. Y.; Weaver, M. J. *J. Phys. Chem. B* **1998**, *102*, 9039.
(17) Grassian, V. H.; Muetterties, E. L. *J. Phys. Chem.* **1987**, *91*, 389.
(18) Kim, Y. G.; Soto, J. E.; Chen, X. L.; Park, Y. S.; Soriaga, M. P. *J. Electroanal. Chem.* **2003**, *554*, 167.
(19) Niwa, S. I.; Eswaramoorthy, M.; Nair, J.; Raj, A.; Itoh, N.; Shoji, H.; Namba, T.; Mizukami, F. *Surf. Sci.* **2002**, *295*, 105.
(20) Netzer, F. P.; Bertel, E.; Matthew, J. A. D. *Surf. Sci.* **1980**, *92*, 43.
(21) Mack, J. U.; Bertel, E.; Netzer, F. P. *Surf. Sci.* **1985**, *159*, 265.
(22) Johnson, K.; Sauerhammer, B.; Titmuss, S.; King, D. A. *J. Chem. Phys.* **2001**, *114*, 9539.
(23) Fischer, T. E.; Kelemen, S. R.; Bonzel, H. P. *Surf. Sci.* **1977**, *64*, 157.
(24) Schmiemann, U.; Baltruschat, H. J. *Electroanal. Chem.* **1993**, *347*, 93.
(25) Montilla, F.; Huerta, F.; Morallon, E.; Vazquez, J. L. *Electrochim. Acta* **2000**, *45*, 4271.
(26) Zebisch, P.; Stichler, M.; Trischberger, P.; Weinelt, M.; Steinruck, H. P. *Surf. Sci.* **1998**, *396*, 61.
(27) Lehwald, S.; Ibach, H.; Demuth, J. E. *Surf. Sci.* **1978**, *78*, 577.
(28) Horsley, J. A.; Stohr, J.; Hitchcock, A. P.; Newbury, D. C.; Johnson, A. L.; Sette, F. *J. Chem. Phys.* **1985**, *83*, 6099.
(29) Somers, J.; Bridge, M. E.; Lloyd, D. R.; Mccabe, T. *Surf. Sci.* **1986**, L167.
(30) Tsai, M. C.; Muetterties, E. L. *J. Am. Chem. Soc.* **1982**, *104*, 2534.
(31) Wander, A.; Held, G.; Hwang, R. Q.; Blackman, G. S.; Xu, M. L.; Andres, P. D.; Van Hove, M. A.; Somorjai, G. A. *Surf. Sci.* **1991**, *249*, 21.
(32) Haq, S.; King, D. A. *J. Phys. Chem.* **1996**, *100*, 16957.
(33) Srinivas, S. T.; Rao, P. K. *J. Catal.* **1994**, *149*, 470.
(34) Rodriguez, J. L.; Pastor, E. *Electrochim. Acta* **2000**, *45*, 4279.
(35) Wan, L. J.; Wang, C.; Bai, C. L.; Osawa, M. *J. Phys. Chem. B* **2001**, *105*, 8399.
(36) Xi, M.; Yang, M. X.; Jo, S. K.; Bent, B. E. *J. Chem. Phys.* **1994**, *101*, 9122.
(37) Munakata, T. *J. Chem. Phys.* **1999**, *110*, 2736.
(38) Howard, M. W.; Cooney, R. P. *Chem. Phys. Lett.* **1982**, *87*, 299.
(39) Wolkow, R. A.; Moskovits, M. *J. Chem. Phys.* **1992**, *96*, 3966.
(40) Litorja, M.; Haynes, C. L.; Haes, A. J.; Jensen, T. R.; Van duyne, R. P. *J. Phys. Chem. B* **2001**, *105*, 6907.
(41) Syomin, D.; Kim, J.; Koel, B. E.; Ellison, G. B. *J. Phys. Chem. B* **2001**, *105*, 8387.
(42) Gao, P.; Weaver, M. J. *J. Phys. Chem.* **1985**, *89*, 5040.
(43) Wijekoon, W. M. K. P.; Koenig, E. W.; Hetherington, W. M., III *J. Phys. Chem.* **1993**, *97*, 1065.
(44) Naaman, R.; Buelow, S. J.; Cheshnovsky, O.; Herschbach, D. R. *J. Phys. Chem.* **1980**, *84*, 2692.
(45) Held, G. *J. Phys.*: *Condens. Matter* **2003**, *15*, R1501.
(46) Duschek, R.; Mittendorfer, F.; Blyth, R. I. R.; Netzer, F. P.; Hafner, J.; Ramsey, M. G. *Chem. Phys. Lett.* **2000**, *318*, 43.
(47) Tomimoto, H.; Takehara, T.; Fukawa, K.; Sumii, R.; Sekitani, T.; Tanaka, K. *Surf. Sci.* **2003**, *5426*, 341.
(48) Sayed, M. B.; Cooney, R. P. *J. Colloid Interface Sci.* **1983**, *91*, 552.
(49) Malherbe, R. R.; Wendelbo, R. *Thermochim. Acta* **2003**, *400*, 165.
(50) Kim, K. W.; Kuppuswamy, M.; Savinell, R. F. *J. Appl. Electrochem.* **2000**, *30*, 543.
(51) Mittendorfer, F.; Hafner, J. *Surf. Sci.* **2001**, *472*, 133.
(52) Lorente, N.; Hedouin, M. F. G.; Palmer, R. E.; Persson, M. *Phys. Rev. B* **2003**, *69*, 155401.
(53) Treboux, G.; Aono, M. *J. Phys, Chem. B* **1997**, *101*, 4620.
(54) Mitendorf, F.; Thomazeau, C.; Raybaud, P.; Toulhoat, H. *J. Phys. Chem. B* **2003**, *107*, 12297.
(55) Morin, C.; Simon, D.; Sautet, P. *J. Phys. Chem. B* **2004**, *108*, 5653.
(56) Morin. C.; Simon, D.; Sautet, P. *J. Phys. Chem. B* **2003**, *107*, 2995.
(57) Saeys, M.; Reyniers, M. F.; Marin, G. B. *J. Phys. Chem. B* **2002**, *106*, 7489.
(58) Saeys, M.; Reyniers, M. F.; Neurock, M.; Marin, G. B. *J. Phys. Chem. B* **2003**, *107*, 3844.
(59) Majumdar, D.; Roszak, S.; Balasubramanian, K. J. *Chem. Phys.* **2001**, *114*, 10300.
(60) Kryachko, E. S.; Arbuznikov, A. V.; Hendrickx, M. F. A. *J. Phys. Chem. B* **2001**, *105*, 3557.
(61) Tian, Z. Q.; Ren, B.; Wu, D. Y. *J. Phys. Chem. B* **2002**, *106*, 9464.
(62) Hu, J. W.; Zhang, Y.; Li, J. F.; Liu, Z.; Ren, B.; Sun, S. G.; Tian, Z. Q.; Lian, T. *Chem. Phys. Lett.* **2005**, *408*, 354.
(63) Liu, G. K.; Yao, J. L.; Ren, B.; Gu, R. A.; Tian, Z. Q. *Electrochem. Commun.* **2002**, *4*, 392.
(64) Liu, G. K.; Ren, B.; Gu, R. A.; Tian, Z. Q. *Chem. Phys. Lett.* **2002**, *364*, 593.
(65) Mrozek, M. F.; Weaver, M. *J. Am. Chem. Soc.* **2002**, *122*, 150.
(66) Tian, Z. Q.; Ren, B. In *Encyclopedia of Electrochemistry*; Bard, A. J., Stratmann, M., Unwin, P. R., Eds.; John Wiley-VCH Verlag GmbH& Co. KGaA: Weinheim, Germany, 2003; p 572.
(67) Cai, W. B.; Ren, B.; Li, X. Q.; She, C. X.; Liu, F. M.; Cai, X. W.; Tian, Z. Q. *Surf. Sci.* **1998**, *406*, 9.
(68) Yao, J. L.; Ren, B.; Liu, G. K.; Wu, D. Y.; Gu, R. A.; Tian, Z. Q. *J. Raman Spectrosc.* **2003**, *34*, 221.
(69) Varsanyi, D. Sc. G. *Assignments for vibrational spectra of seven hundred benzene derivatives*; Akademiai Kiado: Budapest, 1974.
(70) Bernhard, S. *Raman/Infrared Atlas of Organic Compounds*, 2nd ed.; VCH (Weinheim): Weinheim, Germany, 1989.
(71) Liu, G. K.; Duan, S.; Wu, D. Y.; Ren, B.; Gu, R. A.; Tian, Z. Q. To be submitted for publication.
(72) Bugyi, L.; Oszko, A.; Solymosi, F. *Surf. Sci.* **2003**, *539*, 1.
(73) Tauer, T. P.; Sherrill, C. D. *J. Phys. Chem. A* **2005**, *109*, 10475.
(74) Brewer, L. *Science* (*Washington, D.C.*) **1969**, *161*, 115.